

[Click here to view linked References](#)

Authors

Ricardo Gargini^{1**} Berta Segura-Collar^{1†}, María Garranzo-Asensio¹, Rafael Hortigüela^{1,2}, Daniel Lobato-Alonso¹, Miguel Moreno-Raja³, Santiago Esteban³, Juan M. Sepúlveda-Sánchez⁴, Laura Nevola^{3*}, and Pilar Sánchez-Gómez^{1*}

Title

IDP-410: a novel therapeutic peptide that blocks N-MYC over-stability and reduces angiogenesis and tumor progression in glioblastomas

Affiliations

¹Neurooncology Unit, Instituto de Salud Carlos III-UFIEC, Madrid, Spain.

²Current address: Centro de Investigaciones Biológicas Margarita Salas-CSIC, Madrid, Spain

³IDP Discovery Pharma S.L., Barcelona, Spain

⁴Instituto de investigaciones Biomédicas I+12, Hospital 12 de Octubre, Madrid, Spain.

† These authors contributed equally

*To whom correspondence should be addressed:

Ricardo Gargini, rgargini@isciii.es

Pilar Sanchez-Gomez, psanchezg@isciii.es

Laura Nevola, lnevola@idp-pharma.com

Article type: original research

1
2
3
4
5
6
7
8
9
10
11
12
13
14
15
16
17
18
19
20
21
22
23
24
25
26
27
28
29
30
31
32
33
34
35
36
37
38
39
40
41
42
43
44
45
46
47
48
49
50
51
52
53
54
55
56
57
58
59
60
61
62
63
64
65

Competing interests: Laura Nevola and Santiago Esteban are co-founders and shareholders at IDP Discovery Pharma. This work was supported in part by IDP Discovery Pharma funds.

Running title: N-MYC inhibition blocks glioma growth

Summary (150-250 words)

Glioblastomas (GBMs) are the most frequent and highly aggressive brain tumors, being resistant to all cytotoxic and molecularly targeted agents tested so far. There is, therefore, an urgent need to find novel therapeutic approaches and/or alternative targets to bring treatment options to patients. Here, we first show that GBMs express high levels of N-MYC protein, a transcription factor involved in normal brain development. A novel stapled peptide designed to specifically target N-MYC protein monomer, IDP-410, is able to impair the formation of N-MYC/MAX complex and reduce the stability of N-MYC itself. As a result, the viability of GBM cells is compromised. Moreover, the efficacy is found dependent on the levels of expression of N-MYC. Finally, we demonstrate that IDP-410 reduces GBM growth in vivo when administered systemically, both in subcutaneous and intracranial xenografts, reducing the vascularization of the tumors, highlighting a potential relationship between the function of N-MYC and the expression of mesenchymal/angiogenic genes. Overall, our results strengthen the view of N-MYC as a therapeutic target in GBM and strongly suggest that IDP-410 could be further developed to become a first-in-class inhibitor of N-MYC protein, affecting not only tumor cell proliferation and survival, but also the interplay between GBM cells and their microenvironment.

Keywords N-MYC, Peptide Inhibitors, protein stability, Glioblastoma, glioma, tumor microenvironment and angiogenesis.

Introduction

1
2
3 Glioblastoma (GBM), classified as a grade IV astrocytoma, is one of the most
4
5 aggressive forms of cancer, as well as the most frequent malignant primary tumor of
6
7 the brain [1]. Surgical removal of the tumor followed by radiotherapy and
8
9 chemotherapy with temozolomide is the common GBM treatment. However, the
10
11 invasiveness and proliferation rate of tumor cells, as well as their high resistance to
12
13 conventional therapies favor the recurrence of GBM, leading to the death of the
14
15 patients in 15 to 20 months after the first diagnosis [2-4]. The development of new
16
17 types of drugs, especially those capable of reaching the brain, is necessary to
18
19 enhance the survival of these patients, who have not seen a therapeutic
20
21 improvement in the last decades. In this sense, the development of small molecules
22
23 to inhibit the function of transcription factors (TF), as is the case of inhibitors of Brd4
24
25 (Bromodomain containing 4), STAT3 (Signal transducer and activator of transcription
26
27 3), NF κ B (nuclear factor kappa-light-chain-enhancer of activated B cells) or MYC, is
28
29 a major focus of interest in different cancers [5].
30
31
32
33
34
35

36 The MYC family of oncogenes, which includes *c-MYC*, *L-MYC* and *N-MYC*,
37
38 are dysregulated in many neoplasias, associated with poor patients' prognosis [6, 7].
39
40 MYC proteins regulate numerous processes such as cell growth, differentiation and
41
42 apoptosis, normally through dimerization with MYC-associated protein X (MAX) and
43
44 formation of a functional transcriptional activator. However, MYC may also bind MYC
45
46 interacting zinc finger 1, SP1 and other co-factors to repress gene expression [8].
47
48 The transcriptional output signature of MYC proteins is highly dependent on the
49
50 cellular context. L-MYC and N-MYC are distinctly expressed in specific tissues (lung
51
52 and neuronal tissue, respectively), whereas c-MYC is ubiquitously expressed. *c-*
53
54 *MYC* and *N-MYC* can replace each other during normal development [9] or in cancer,
55
56 where they often show mutually exclusive expression patterns [10] [11].
57
58
59
60
61
62
63
64
65

1
2
3
4
5
6
7
8
9
10
11
12
13
14
15
16
17
18
19
20
21
22
23
24
25
A two-fold rise in MYC levels suffices to affect cell cycle progression, leading to cancer [12], so the expression of this TF is tightly regulated. Proliferating cells allow for MYC stabilization at a protein level, but quiescent cells degrade the protein through the ubiquitin degradation pathway, a process that depends on the phosphorylation status of MYC proteins [13]. Indeed, overexpression of N-MYC harboring a mutation at threonine 58 that leads to protein stability can originate cerebellar medulloblastomas as well as forebrain gliomas [14]. Direct amplification or overexpression of *MYC* genes have also been found in human brain tumors, including pediatric gliomas, adult GBM and medulloblastomas [13, 15-19]. Moreover, different oncogenic alterations promote the tumorigenicity of glioma stem cells through c-MYC stabilization [20, 21].

26
27
28
29
30
31
32
33
34
35
36
37
38
39
40
41
42
43
44
45
46
47
48
49
MYC proteins are considered undruggable because they belong to the internally disordered proteins (IDPs) group, which lack a stable 3D structure and exist instead as ensembles of rapidly interchanging conformations [22]. On top of that, their intra-nuclear localization supposes an additional challenge. Still, many efforts have been made over the last years to target MYC genes to treat different cancer types, including inhibiting MYC transcription or transcriptional activity, protein stability, dimerization, immune therapy, and synthetic lethality [23-27]. These have allowed establishing the important role of N-MYC in medulloblastomas and neuroblastomas [13]. However, specific downregulation or inhibition of this gene has not been tested yet in GBMs.

50
51
52
53
54
55
56
57
58
59
60
61
62
63
64
65
In this work, we confirm the strong expression of N-MYC in human GBM samples and mouse models. Notably, no increase is observed in the amount of *MYCN* mRNA. Moreover, we describe the anti-glioma effect of IDP-410, a stapled peptide specifically designed to target N-MYC. By using primary glioma cell lines, we demonstrate that this novel inhibitor reduces the viability of those cells expressing

1 high levels of this TF. IDP-410 disrupts the N-MYC-MAX complex, reducing the
2 stability of N-MYC protein and the amount of nuclear staining. Systemic treatment
3
4 with IDP-410 reduces heterotopic and orthotopic glioma growth by attenuating the
5
6 vascularization of the tumors. Our results show a potential relationship between the
7
8 function of N-MYC and the expression of mesenchymal/angiogenic genes. Overall,
9
10 the results presented here suggest that IDP-410 could be a first-in-class inhibitor of
11
12 N-MYC in GBM, affecting the interplay between the tumor cells and their
13
14 microenvironment.
15
16
17
18
19
20
21

22 **Materials and Methods**

23 **Human samples**

24
25
26
27
28 Normal tissue (NT) was obtained postmortem from non-pathological brain samples.
29
30 NT and glioma samples (fresh frozen or embedded in paraffin) were obtained after
31
32 patient's written consent and with the approval of the Ethical Committee at Hospital
33
34 12 de Octubre (Madrid, Spain) (CEI 14/023 and CEI 18/024). The primary cell lines
35
36 (Supplementary Table S1) were generated as previously described [28]. They belong
37
38 to the Biobank of Hospital 12 de Octubre. They were maintained in stem cell medium
39
40 (Neurobasal (Invitrogen) supplemented with B27 (1:50) (Invitrogen); GlutaMAX
41
42 (1:100) (Invitrogen); penicillin-streptomycin (1:100) (Lonza); 0.4% heparin (Sigma-
43
44 Aldrich); and 40 ng/ml EGF and 20 ng/ml bFGF2 (Peprotech)) and passaged after
45
46 enzymatic disaggregation using Accumax (Millipore).
47
48
49
50
51

52 **IDP-410 synthesis and characterization.**

53
54 The linear peptide was synthesized with automatic synthesizer using 9-
55
56 fluorenylmethoxycarbonyl/tertbutyl solid phase peptide chemistry. Ring-closing
57
58 metathesis reaction was performed in solution with a first-generation Grubbs catalyst
59
60
61
62
63
64
65

1 after cleaving the linear peptide from the resin, as previously described (Scott J.M. et al.,
2 “Application of Ring-Closing Metathesis to the Synthesis of Rigidified Amino Acids and
3 Peptides”, 1996, J. Am. Chem. Soc., 1996, 118 (40), pp 9606–9614). The compound was
4 purified by HPLC-RP (C-18 column; Pump A: H₂O with 0,1% TFA; Pump B Acetonitrile
5 with 0,1% TFA) using a linear gradient 44%-54% of B in 15 minutes (purity grade 95%
6 by HPLC) and identified by ESI-MS.
7
8
9
10
11
12

13 **In vitro treatments**

14 The stock solution of IDP-410 (IDP Discovery pharma) was prepared at 10mM in
15 PBS. For viability assays, 5000 cells were seeded in triplicate wells of a 96-well
16 microplate coated with matrigel (Bekton-Dickinson, 15mg/ml stock solution diluted
17 1:100 in DMEM medium (Lonza)). 24h later, cells were treated with IDP-410 (at the
18 indicated concentrations in each assay) and viability was measured after 72h of
19 treatment. For that, cells were incubated with Hoechst 33342 (1:200, Sigma-Aldrich)
20 and propidium iodide (1:1000, Merck) and fluorescence was measured in a Cytell
21 Cell Imaging System (GE Healthcare Life Sciences). Wells containing non-treated
22 cells were considered as 100% viability for each tested cell line.
23
24
25
26
27
28
29
30
31
32
33
34
35
36

37 For the N-MYC degradation experiment, GBM6 and GBM7 cells were grown in
38 presence of DMSO or MG132 (Millipore) 10 µM for 1h and then the cells were
39 incubated with IDP-410 (10 µM) for 6h. Then, cells were collected and lysed and
40 subsequently analyzed by western blot, as described below.
41
42
43
44
45
46

47 **Wound healing assay**

48 HBMEC cells were seeded at a density of 5×10^5 cells per well into 24-well flat-
49 bottom microplates and incubated in 10% FBS-supplemented DMEM until sealed.
50 Then, the wound was performed by scratching across the bottom of the well using a
51 pipette tip. Medium was removed and cells were washed with PBS prior to adding
52 the conditioned medium (CM). Glioma CM was obtained by incubating GBM6 cells
53
54
55
56
57
58
59
60
61
62
63
64
65

1
2
3
4
5
6
7
8
9
10
11
12
13
14
15
16
17
18
19
20
21
22
23
24
25
26
27
28
29
30
31
32
33
34
35
36
37
38
39
40
41
42
43
44
45
46
47
48
49
50
51
52
53
54
55
56
57
58
59
60
61
62
63
64
65

for 48h in presence of 5µM IDP-410 or PBS. After 48 h, the medium was removed and replaced with fresh starving medium for 6h. Then, CM was collected, briefly spun and the supernatant was used for the wound-healing assays. To calculate wound-closing rate, pictures were taken at different times and wound area was measured as square pixels using ImageJ.

In vivo assays

Animal experiments were reviewed and approved by the Research Ethics and Animal Welfare Committee at our institution (Instituto de Salud Carlos III, Madrid) (PROEX 244/14 and 02/16), in agreement with the European Union and national directives. For subcutaneous transplantations, cells (3×10^6) were resuspended 1:1 in culture media and Matrigel (BD) and then subcutaneously injected into athymic nude Foxn1nu mice (Harlan Iberica). When the tumors reached a visible size, we started measuring them with a caliper. At that point, animals started receiving IDP-410 at 15 mg/kg through intravenous (i.v) injections (twice a week). Control animals were treated with the PBS solvent. 2h before sacrifice, the animals received intraperitoneal injections of 5-Bromo-2'-deoxyuridine (BrdU) (Sigma Aldrich) (50mg/Kg) in saline solution.

To establish the intracranial tumors, we injected 100.000 GBM6 cells (resuspended in 2 µl of culture stem cell medium) with a Hamilton syringe into Nude mice. The injections were made into the striatum (coordinates: A–P, –0.5 mm; M–L, +2 mm, D–V, –3 mm; related to Bregma) using a Stoelting Stereotaxic device. Two weeks after the tumor implantation, we started treating the animals. For that, IDP-410 was dissolved in PBS+1% Polysorbate and injected subcutaneously (15/mg/Kg/day). Control animals were treated with this solvent. Tumor growth was monitored in an IVIS equipment (Perkin Elmer) after intraperitoneal injection of D-luciferin (75 mg/kg;

1 PerkinElmer). Animals were sacrificed when they showed signs of disease and the
2 brains were processed for cellular and molecular analysis.
3
4

5 **Quantitative reverse-transcriptase PCR (qRT-PCR)**

6

7
8 RNA was extracted from the tissue or the cell pellets using RNA isolation Kit (Roche)
9 and it was digested with DNase I (Roche) according to the manufacturer's
10 instructions. cDNA was synthesized with SuperScript II Reverse Transcriptase
11 (Takara). Quantitative real time PCR (qRT-PCR) reactions were performed using the
12 Light Cycler 1.5 (Roche) with the SYBR Premix Ex Taq (Takara). The primers used
13 for each reaction are indicated in Supplementary Table S2. Gene expression was
14 quantified by the double delta Ct method.
15
16
17
18
19
20
21
22
23
24

25 **Immunofluorescent (IF) and Immunohistochemical (IHC) staining and** 26 **quantification**

27

28
29 Tumor tissues were embedded in paraffin and cut with a microtome. The slides were
30 heated at 60°C for 1 hour followed by deparaffinization and hydration, washed with
31 water, placed into antigen retrieval solution (pressure-cooking) in 10 mM sodium
32 citrate pH 6.0. Paraffin sections were permeabilized with 1% Triton X-100 (Sigma-
33 Aldrich) in PBS and blocked for 1 hour in PBS with 5% BSA (Sigma), 10% FBS
34 (Sigma) and 0,1% Triton X-100 (Sigma). For the detection of ki67 or BrdU, sections
35 were incubated with pre-heated 2N HCl for 15 min, followed by 10 min incubation
36 with 0,1 M sodium borate pH 8,5, and then continued with the blocking solution as
37 described above. The following primary antibodies (Supplementary Table S3) were
38 incubated O/N at 4°C. The second day, sections were washed with PBS three times
39 prior to incubation with the appropriate secondary antibody (Supplementary Table
40 S3) for 2h at room temperature. Prior to coverslip application, nuclei were
41 counterstained with DAPI. Imaging was done with Leica SP-5 confocal microscope.
42
43
44
45
46
47
48
49
50
51
52
53
54
55
56
57
58
59
60
61
62
63
64
65

1
2
3
4
5
6
7
8
9
10
11
12
13
14
15
16
17
18
19
20
21
22
23
24
25
26
27
28
29
30
31
32
33
34
35
36
37
38
39
40
41
42
43
44
45
46
47
48
49
50
51
52
53
54
55
56
57
58
59
60
61
62
63
64
65

Otherwise, IHC sections were incubated with biotinylated secondary antibodies (1:200 dilution). Target proteins were detected with the ABC Kit and the DAB kit (Vector Laboratories).

For quantification, slides were scanned at 63X or 40X magnification. The number of BrdU-positive cells per field was counted with Fiji-ImageJ software and normalized with the total number of cells. For the quantification of the vasculature, we counted the number of dilated vessels per field, substrated from endomucin IHC.

Western Blot (WB) analysis

Protein extracts were prepared by re-suspending cell pellets or tumor tissue samples in lysis buffer (50 mM Tris (pH 7.5), 300 mM NaCl, 0.5% SDS, and 1% Triton X-100) and incubating the cells for 15 min at 100°. The lysed extracts were centrifuged at 13,000 g for 10 min at room temperature and the protein concentration was determined using a commercially available colorimetric assay (BCA Protein Assay Kit). Approximately 30 µg of protein were resolved by 10% or 12% SDS-PAGE and they were then transferred to a nitrocellulose membrane (Hybond-ECL, Amersham Biosciences). The membranes were blocked for 1 h at room temperature in TBS-T (10 mM Tris-HCl (pH 7.5), 100 mM NaCl, and 0.1% Tween-20) with 5% skimmed milk, and then incubated overnight at 4°C with the corresponding primary antibody (Supplementary Table S3) diluted in TBS-T. After washing 3 times with TBS-T, the membranes were incubated for 2 h at room temperature with their corresponding secondary antibody (Supplementary Table S3) diluted in TBS-T. Proteins were visible by enhanced chemiluminescence with ECL (Pierce) using Amersham imager 680 and the signal was quantified by Fiji-ImageJ software.

Immunoprecipitation

1 GBM6 cells were incubated in the presence of DMSO or IDP-410 (5 μ M) for 6h. Then,
2 the cells were collected, washed in PBS and the protein extracts were generated
3 in ice-cold lysis buffer (50 mM Tris-HCl [pH 7.6], 150 mM NaCl, 1% Triton X100,
4 0.5% sodium deoxycholate, 1 mM phenylmethylsulfonyl fluoride, 1 μ g/ml leupeptin)
5 during 30 min. After that, the extracts were pre-cleared for 1 hr with Protein A/G-
6 Sepharose (Santa Cruz Biotechnology, Inc.) and immunoprecipitated (IP) using anti-
7 N-MYC antibodies (Cell signaling) or IgG as a control. The IP fractions were analyzed
8 by WB with N-MYC (Santa Cruz Biotech) and MAX (Cell signaling) antibodies.
9
10
11
12
13
14
15
16
17
18
19

20 **In silico analysis**

21
22
23 The Cancer Genome Atlas (TCGA) GBM dataset was accessed via UCSC xena-
24 browser (<https://xenabrowser.net>) for extraction of N-MYC gene's expression level.
25
26
27

28 **Statistical Analysis**

29
30
31 GraphPad Prism 5 software was used for data presentation and statistical analysis.
32
33 For bar graphs, the level of significance was determined by a two-tailed un-paired
34 Student's t-test. The difference between experimental groups was assessed by
35 Paired t-Test and one-way ANOVA. To analyze the survival of nude mice, we used
36 the Kaplan–Meier method and evaluated with a two-sided log-rank test. For
37 correlation analysis between each gene, expression data were tested by Pearson's
38 correlation coefficient and Spearman's correlation coefficient. P values < 0.05
39 were considered significant (*p < 0.05; **p < 0.01; *** p< 0.001; **** p< 0.0001; n.s.,
40 non-significant). All quantitative data presented are the mean \pm SEM.
41
42
43
44
45
46
47
48
49
50
51
52
53
54
55
56
57
58
59
60
61
62
63
64
65

Results

N-MYC is highly expressed in gliomas

To evaluate whether N-MYC is dysregulated in glioblastoma cell lines, we first studied its presence by quantifying its RNA levels. We did not find an increase in *N-MYC* transcription in GBM samples compared to normal brain, both in our cohort (Fig. 1a) or in the analysis of TCGA samples (RNAseq or microarray data) (Supplementary Fig. 1a-b). By contrast, using protein extracts from patients' samples we observed a clear upregulation of N-MYC protein in GBMs compared to non-tumor (NT) tissues (Fig. 1b and c). Some of the patient derived xenografts (PDX) also express high levels of N-MYC protein (Fig. 1d), with frequent nuclear staining in the mouse tumors (Fig. 1e) and a strong consistency between the WB and the IF quantification (Fig. 1f). These results confirm the increased levels of N-MYC protein in GBM and suggest that the main mechanisms for this upregulation must be related to increased translation and/or stabilization of the protein.

Effect of IDP-410 N-MYC inhibition in glioma growth in vitro

We studied IDP-410, a novel stapled peptide designed to specifically target and inhibit the function of N-MYC, as therapeutic agent in GBM, its mechanism of action and the biological consequences of inhibiting N-MYC in vitro. For that, we first analyzed the levels of expression of N-MYC in a battery of primary GBM cell lines (Fig. 2a). The exposure of GBM6 (high N-MYC expression) to increasing concentrations of IDP-410 clearly reduced the viability of the cells (Fig. 2b). Moreover, 10 μ M of IDP-410 triggered the cell death of all the primary cell lines expressing high levels of N-MYC (Fig. 2c). By contrast, there was very little effect of this compound in GBM8, GBM10 or fibroblasts, which express reduced amounts of

1 N-MYC (Fig. 2c). A direct comparison of the effect of IDP-410 in GBM6 (high N-
2 MYC), GBM2 (low N-MYC) and fibroblasts (no N-MYC) (Fig. 2d) showed the strong
3 correlation between the expression of the target and the sensitivity to the drug (Fig.
4 2e), reinforcing its specificity.
5
6
7
8
9

10 ***IDP-410 induces N-MYC protein degradation in vitro and disrupts N-MYC/MAX*** 11 ***complex*** 12 13 14 15 16

17 The incubation of GBM6 cells with increasing amounts of IDP-410 for 6 hours
18 reduced the amount of N-MYC protein in the cells (Fig. 3a-b). Notably, the enhanced
19 degradation induced by IDP-410 was blocked in the presence of the proteasome
20 inhibitor MG132, both in GBM6 and GBM7 cells (Fig. 3c-e). We also observed an
21 impairment of N-MYC and MAX interaction in the presence of IDP-410 (Fig. 3f).
22 Taking together, these results suggest that the IDP-410 inhibitory effect is associated
23 with the dissociation of the N-MYC/MAX complex and the degradation of N-MYC.
24
25
26
27
28
29
30
31
32
33
34
35
36
37

38 ***IDP-410 suppresses glioma growth in vivo*** 39 40

41 To evaluate whether the effect of IDP-410 observed in vitro translates to an
42 in vivo setting, we injected GBM6 cells subcutaneously in immunodeficient mice and
43 treated the animals intravenously (i.v.) with IDP-410. The growth curve of the tumors
44 shows that systemic treatment with IDP-410 reduced significantly the tumor size, in
45 comparison to vehicle (PBS) (Fig. 4a-b). Immunofluorescence staining of tissues
46 from both sets of mice demonstrated a reduced nuclear N-MYC expression after IDP-
47 410 treatment (Fig. 4c). Furthermore, BrdU incorporation was reduced in IDP-410
48 treated mice in comparison with control tumors (Fig. 4d-e), whereas the percentage
49 of apoptotic cells (measured through activated Caspase 3 staining) was not different
50
51
52
53
54
55
56
57
58
59
60
61
62
63
64
65

1
2
3
4
5
6
7
8
9
10
11
12
13
14
15
16
17
18
19
20
21
22
23
24
25
26
27
28
29
30
31
32
33
34
35
36
37
38
39
40
41
42
43
44
45
46
47
48
49
50
51
52
53
54
55
56
57
58
59
60
61
62
63
64
65

between the two groups of mice (Supplementary Fig. 2). These results suggest that N-MYC inhibition impairs the growth of GBM tumors but does not promote cell death in immune-supressed, tumor bearing mice xenografts.

To determine if IDP-410 is able to cross the blood brain barrier and block the growth of orthotopic gliomas, we injected GBM6 cells into the brain of Nude mice. Two weeks later, we started treating the animals with vehicle (Polisorbate 1% in PBS) or IDP-410, injected subcutaneously. As the cells express the luciferase reporter, we were able to follow up tumor progression in situ and we determined that IDP-410 reduced the growth of GBM6 cells (Fig. 5a). Moreover, it increases the survival of the tumor-bearing animals (Fig. 5b). The analysis of the excised tumors showed a strong downregulation of nuclear N-MYC in IDP-410 treated samples (Fig. 5c) and a decrease in the amount of N-MYC protein, measured by WB (Fig. 5d). In agreement with the results obtained in the heterotopic tumor setting, the amount of proliferative cells in the intracranial tumors was also diminished after systemic IDP-410 treatment (Fig. 5e). Altogether, these results suggest that the IDP-410 reaches the brain, decreases the stability of N-MYC protein and inhibits the growth of GBM cells.

IDP-410 affects tumor proliferation and vascularization in treated mice

MYC proteins regulate the crosstalk between the tumor and the host and have been linked to processes of proliferation and angiogenesis [29-31]. To explore the possible anti-tumor mechanisms of N-MYC inhibition by IDP-410, we selected a series of 27 genes known to be regulated by N-MYC and mainly associated with these two processes (Fig. 6a). We observed that the mRNA expression of some of these genes was reduced when GBM6 and GBM3 cells were cultured in the presence of IDP-410 (Fig. 6b and c). Notably, a very similar inhibition pattern was observed in

1 the intracranial GBM6 tumors after systemic IDP-410 treatment (Fig. 6d).
2 Furthermore, we confirmed that the expression of important angiogenesis- (*VEGFA*,
3 *VEGF*) and proliferation- (*MIK67*, *Ki67*) related genes correlated positively with N-
4 MYC protein levels in a panel of glioma PDXs (Fig. 6e and f; Supplementary Fig. 3).
5
6
7
8
9

10 It is well known that glioma cells, particularly in high-grade tumors, express a
11 variety of genes that promote different steps of the angiogenesis process [32]. To
12 study if N-MYC inhibition by IDP-410 could affect this pro-angiogenic function of
13 gliomas, we first performed an in vitro assay using GBM6 cells. We examined the
14 effect of conditioned media (CM) from these glioma cells (treated or not with IDP-
15 410) on the wound healing capacity of HBMEC cells. Fig. 7 a-b shows that treatment
16 with IDP-410 impaired the effect of glioma CM on the endothelial migration of
17 HBMEC cells.
18
19
20
21
22
23
24
25
26
27
28

29 We have recently shown that mesenchymal transformation is key to induce
30 angiogenesis in GBM, even for the generation of tumor blood vessels [33]. When we
31 characterized the tumor tissue from IDP-410 treated animals, we observed a clear
32 reduction on the amount of TAZ and α SMA, which are mesenchymal-related proteins
33 [34], in comparison with control samples (Fig. 7c). Moreover, we observed that IDP-
34 410 treated tumors contained reduced levels of the angiogenic factor VEGF (Fig.
35 7d). In addition, the IHC staining with endomucin antibodies showed a strong
36 reduction in the number of dilated blood vessels in the presence of IDP-410 (Fig. 7e).
37 Taken together, our results suggest that the anti-tumor effect of N-MYC inhibition by
38 IDP-410 is mediated, at least in part, by the decrease in tumor-cell proliferation and
39 by the reduction of neo-vascularization processes.
40
41
42
43
44
45
46
47
48
49
50
51
52
53
54
55
56
57
58
59
60
61
62
63
64
65

Discussion

1
2
3 GBM is one of the deadliest tumor types with a very short life expectancy upon
4 diagnosis. Its treatment does not succeed mainly because of its highly
5 heterogeneous and plastic nature [35]. Thus, there is an urgent need to search for
6 new therapeutic strategies. MYC proteins are one of the most wanted targets due to
7 their notorious oncogenic features [5, 6, 23, 26]. However, a long standing
8 consideration for the clinical development of MYC inhibitors is the potential side
9 effects due to its capacity to regulate proliferation in normal tissues. Indeed, systemic
10 inhibition of Myc in transgenic mice models for continuous long periods (4 weeks)
11 was shown to affect high proliferating tissues, such as skin and gastrointestinal tract,
12 but found to be well tolerated, not to alter the homeostasis of the tissues, and the
13 effect readily reversed when Myc was reactivated [36]. In that sense, targeting
14 specifically N-MYC, with a more neural-restricted pattern of expression, has become
15 of interest for many pediatric cancers but also for certain adult neoplasia, including
16 GBM [24].
17
18
19
20
21
22
23
24
25
26
27
28
29
30
31
32
33
34
35

36 Here, we have confirmed the overexpression of *N-MYC* gene compared to
37 normal tissue in a percentage of human GBM samples and PDXs. Interestingly, we
38 found no correlation between the levels of protein and mRNA. This suggest that
39 protein stabilization is an important regulatory event and that *N-MYC* transcriptional
40 data cannot be used to evaluate the overexpression of N-MYC protein in gliomas
41 [19]. More importantly, we show here compelling evidence supporting the anti-tumor
42 effect of a novel stapled peptide IDP-410 specifically designed to target N-MYC in
43 those GBM expressing high levels of N-MYC, both in vitro and in vivo. These results
44 demonstrate the therapeutic potential of IDP-410, which shows capacity to reach
45 subcutaneous and intracranial tumors when administered systemically, with high
46
47
48
49
50
51
52
53
54
55
56
57
58
59
60
61
62
63
64
65

1
2
3
4
5
6
7
8
9
10
11
12
13
14
15
16
17
18
19
20
21
22
23
24
25
26
27
28
29
30
31
32
33
34
35
36
37
38
39
40
41
42
43
44
45
46
47
48
49
50
51
52
53
54
55
56
57
58
59
60
61
62
63
64
65

tollerability. Moreover, the data suggest that N-MYC (protein, not mRNA) should be used as a biomarker of response to IDP-410.

The nuclear localization of MYC proteins and their intrinsically disordered structure hampers the development of classical small molecule inhibitors against these TFs. Strategies to impair MYC protein function via its transcription and protein or mRNA stability have been developed and some of them have reached the clinic [5, 23, 26, 27]. The most recent example is Omomyc, a miniprotein analog to cMYC currently in Phase I for treatment of solid tumors (NCT04808362). It was shown that Omomyc, when conditionally expressed in transgenic models, antagonizes the function of MYC family members and reduce the growth of different types of cancer including GBMs [26]. When administered systemically and intranasally, Omomyc was shown to inhibit tumor growth in lung cancer animal models [37]. However, its potential to reach the brain and act against gliomas has not been evaluated [38].

Our results show that the IDP-410 peptide acts by reducing the interaction of N-MYC with its partner MAX and favoring the degradation of the protein. Systemic IDP-410 treatment induced a decrease in cell proliferation and a clear inhibition of glioma vascularization. In agreement with that, IDP-410 reduce the pro-angiogenic properties of glioma cells in vitro. As a possible mechanism to explain this effect, we observed a strong downregulation of *VEGFA* expression in tumors treated with IDP-410. Moreover, we show a significant correlation between *VEGFA* transcription and the amount of N-MYC protein in GBM xenografts. *VEGFA*, which is normally secreted by tumor cells, is a key player in angiogenesis as it binds to the endothelial VEGFR2 and promotes proliferation and migration, leading to new vessel-like structures [39-41]. Therefore, our results suggest for the first time a direct regulation of GBM angiogenesis by N-MYC inhibition through the modulation of the expression of *VEGFA* and possibly other vascular-related molecules. This is in agreement with the

1 widely accepted role of c-MYC as a modulator of different aspects of the tumor
2 microenvironment, including the vasculature [29, 42] and with the correlation of *N-*
3 *MYC* amplification with angiogenesis in neuroblastoma [43].
4
5
6

7 High-grade gliomas are extremely dependent on their vascular
8 microenvironment, which allows the tumor to gather needed nutrients and oxygen for
9 its growth and promotes the progression of the disease. Florid angiogenesis is
10 associated with the appearance of mesenchymal features, which is linked to the
11 aggressiveness of gliomas [33]. Furthermore, tumor cells that have become
12 mesenchymal invade the adjacent parenchyma or may even interact with endothelial
13 cells, a property that allows them to govern the brain vasculature [44]. Our recent
14 results indicate that these processes are mediated by increases in TAZ and α -SMA
15 expression in glioma cells [33, 45]. Moreover, tumor TAZ activation is often correlated
16 with increased levels of angiogenesis while endothelial TAZ activation is needed for
17 the formation of blood and lymphatic vessels [46]. In addition, this transcription factor
18 controls the mesenchymal transformation of gliomas, which is associated with
19 changes in the tumor microenvironment [47]. The expression analysis in tumors
20 treated with IDP-410 suggest a reduction in the mesenchymal features of gliomas
21 after *N-MYC* inhibition. We propose here that this change in tumor phenotype, added
22 to the *VEGFA* decrease, might reduce the vascularization and the growth of the
23 tumors.
24
25
26
27
28
29
30
31
32
33
34
35
36
37
38
39
40
41
42
43
44
45
46

47 Overall, our data highlights the relevance of *N-MYC* in glioma pathology, and
48 in particular its role via the over-stabilization of the protein. Moreover, we have
49 demonstrated the efficacy and mechanism of action of IDP-410, a newly designed
50 peptide that targets directly *N-MYC* protein. Although the results obtained shed some
51 hope for a possible GBM stratified treatment, more insight into IDP-410's effects
52 need to be gathered. Especially interesting would be to study the effect of IDP-410
53
54
55
56
57
58
59
60
61
62
63
64
65

1
2
3
4
5
6
7
8
9
10
11
12
13
14
15
16
17
18
19
20
21
22
23
24
25
26
27
28
29
30
31
32
33
34
35
36
37
38
39
40
41
42
43
44
45
46
47
48
49
50
51
52
53
54
55
56
57
58
59
60
61
62
63
64
65

in the immune component of the microenvironment and its combination with immune checkpoint inhibitors in GBM tumors, as MYC inhibitors can enhance the anti-tumoral immune response [48]. Moreover, combinatorial approaches with anti-angiogenic molecules, which have failed to block GBM growth [49], would be desirable. In any case, the results presented here shows the great therapeutic potential of IDP-410 in GBM as it disrupts the supportive tumor microenvironment, which is probably less susceptible to the appearance of resistant subclones with different genetic alterations.

Acknowledgements

This work was supported by Ministerio de Economía y Competitividad: (Acción Estratégica en Salud) and FEDER funds: PI16/01550 to JMS, by “Asociación Española contra el Cancer grants: INVES192GARG to RG, GCTRA16015SEDA to JMS and IDEAS20095SÁNC to PSG, and by Ministerio de Ciencia, Innovación y Universidades and FEDER funds: RTI2018-093596 to PSG. MGA was supported by the Young Employment Initiative (Comunidad de Madrid).

References

1. Louis DN, Perry A, Reifenberger G, von Deimling A, Figarella-Branger D, Cavenee WK, et al. The 2016 World Health Organization Classification of Tumors of the Central Nervous System: a summary. *Acta Neuropathol.* 2016;131(6):803-20. doi: 10.1007/s00401-016-1545-1.
2. Nieder C, Adam M, Molls M, Grosu AL. Therapeutic options for recurrent high-grade glioma in adult patients: recent advances. *Critical reviews in oncology/hematology.* 2006;60(3):181-93. doi: 10.1016/j.critrevonc.2006.06.007.
3. Stupp R, Mason WP, van den Bent MJ, Weller M, Fisher B, Taphoorn MJ, et al. Radiotherapy plus concomitant and adjuvant temozolomide for glioblastoma. *The New England journal of medicine.* 2005;352(10):987-96. doi: 10.1056/NEJMoa043330.
4. Wong ML, Kaye AH, Hovens CM. Targeting malignant glioma survival signalling to improve clinical outcomes. *J Clin Neurosci.* 2007;14(4):301-8. doi: 10.1016/j.jocn.2006.11.005.
5. Chen A, Koehler AN. Transcription Factor Inhibition: Lessons Learned and Emerging Targets. *Trends Mol Med.* 2020;26(5):508-18. doi: 10.1016/j.molmed.2020.01.004.
6. Albiñá A, Johnsen JI, Henriksson MA. MYC in oncogenesis and as a target for cancer therapies. *Adv Cancer Res.* 2010;107:163-224. doi: 10.1016/s0065-230x(10)07006-5.
7. Carroll PA, Freie BW, Mathsyaraja H, Eisenman RN. The MYC transcription factor network: balancing metabolism, proliferation and oncogenesis. *Front Med.* 2018;12(4):412-25. doi: 10.1007/s11684-018-0650-z.
8. Lourenco C, Resetca D, Redel C, Lin P, MacDonald AS, Ciaccio R, et al. MYC protein interactors in gene transcription and cancer.
9. Malynn BA, de Alboran IM, O'Hagan RC, Bronson R, Davidson L, DePinho RA, et al. N-myc can functionally replace c-myc in murine development, cellular growth, and differentiation. *Genes & development.* 2000;14(11):1390-9.
10. Westermann F, Muth D, Benner A, Bauer T, Henrich K-O, Oberthuer A, et al. Distinct transcriptional MYCN/c-MYC activities are associated with spontaneous regression or malignant progression in neuroblastomas. *Genome Biology.* 2008;9(10):R150. doi: 10.1186/gb-2008-9-10-r150.
11. Northcott PA, Shih DJ, Peacock J, Garzia L, Morrissy AS, Zichner T, et al. Subgroup-specific structural variation across 1,000 medulloblastoma genomes. *Nature.* 2012;488(7409):49-56. doi: 10.1038/nature11327.
12. Bretones G, Delgado MD, León J. Myc and cell cycle control. *Biochim Biophys Acta.* 2015;1849(5):506-16. doi: 10.1016/j.bbagr.2014.03.013.
13. Borgenvik A, Cancer M, Hutter S, Swartling FJ. Targeting MYCN in Molecularly Defined Malignant Brain Tumors. *Front Oncol.* 2020;10:626751. doi: 10.3389/fonc.2020.626751.
14. Swartling FJ, Savov V, Persson AI, Chen J, Hackett CS, Northcott PA, et al. Distinct neural stem cell populations give rise to disparate brain tumors in response to N-MYC. *Cancer Cell.* 2012;21(5):601-13. doi: 10.1016/j.ccr.2012.04.012.
15. Faria MH, Khayat AS, Burbano RR, Rabenhorst SH. c-MYC amplification and expression in astrocytic tumors. *Acta Neuropathol.* 2008;116(1):87-95. doi: 10.1007/s00401-008-0368-0.
16. Orian JM, Vasilopoulos K, Yoshida S, Kaye AH, Chow CW, Gonzales MF. Overexpression of multiple oncogenes related to histological grade of astrocytic glioma. *British journal of cancer.* 1992;66(1):106-12. doi: 10.1038/bjc.1992.225.
17. Herms JW, von Loewenich FD, Behnke J, Markakis E, Kretschmar HA. c-myc oncogene family expression in glioblastoma and survival. *Surg Neurol.* 1999;51(5):536-42. doi: 10.1016/s0090-3019(98)00028-7.
18. Hui AB, Lo KW, Yin XL, Poon WS, Ng HK. Detection of multiple gene amplifications in glioblastoma multiforme using array-based comparative genomic hybridization. *Lab Invest.* 2001;81(5):717-23. doi: 10.1038/labinvest.3780280.

19. Hodgson JG, Yeh RF, Ray A, Wang NJ, Smirnov I, Yu M, et al. Comparative analyses of gene copy number and mRNA expression in glioblastoma multiforme tumors and xenografts. *Neuro Oncol.* 2009;11(5):477-87. doi: 10.1215/15228517-2008-113.
20. Zheng H, Ying H, Yan H, Kimmelman AC, Hiller DJ, Chen AJ, et al. p53 and Pten control neural and glioma stem/progenitor cell renewal and differentiation. *Nature.* 2008;455(7216):1129-33. doi: 10.1038/nature07443.
21. Fukasawa K, Kadota T, Horie T, Tokumura K, Terada R, Kitaguchi Y, et al. CDK8 maintains stemness and tumorigenicity of glioma stem cells by regulating the c-MYC pathway. *Oncogene.* 2021;40(15):2803-15. doi: 10.1038/s41388-021-01745-1.
22. Fuertes G, Nevola L, Esteban-Martín S. Chapter 9 - Perspectives on drug discovery strategies based on IDPs. In: Salvi N, editor. *Intrinsically Disordered Proteins.* Academic Press; 2019. p. 275-327.
23. McAnulty J, DiFeo A. The Molecular 'Myc-anisms' Behind Myc-Driven Tumorigenesis and the Relevant Myc-Directed Therapeutics. *International journal of molecular sciences.* 2020;21(24). doi: 10.3390/ijms21249486.
24. Liu Z, Chen SS, Clarke S, Veschi V, Thiele CJ. Targeting MYCN in Pediatric and Adult Cancers. *Front Oncol.* 2020;10:623679. doi: 10.3389/fonc.2020.623679.
25. Wang C, Zhang J, Yin J, Gan Y, Xu S, Gu Y, et al. Alternative approaches to target Myc for cancer treatment. *Signal Transduct Target Ther.* 2021;6(1):117. doi: 10.1038/s41392-021-00500-y.
26. Whitfield JR, Beaulieu ME, Soucek L. Strategies to Inhibit Myc and Their Clinical Applicability. *Front Cell Dev Biol.* 2017;5:10. doi: 10.3389/fcell.2017.00010.
27. Bayliss R, Burgess SG, Leen E, Richards MW. A moving target: structure and disorder in pursuit of Myc inhibitors. *Biochem Soc Trans.* 2017;45(3):709-17. doi: 10.1042/bst20160328.
28. Pozo N, Zahonero C, Fernandez P, Linares JM, Ayuso A, Hagiwara M, et al. Inhibition of DYRK1A destabilizes EGFR and reduces EGFR-dependent glioblastoma growth. *Journal of Clinical Investigation.* 2013;123(6):2475-87. doi: 10.1172/JCI63623.
29. Meškytė EM, Keskas S, Ciribilli Y. MYC as a Multifaceted Regulator of Tumor Microenvironment Leading to Metastasis. *Int J Mol Sci.* 2020;21(20). doi: 10.3390/ijms21207710.
30. Chantry YH, Gustafson WC, Itsara M, Persson A, Hackett CS, Grimmer M, et al. Paracrine signaling through MYCN enhances tumor-vascular interactions in neuroblastoma. *Sci Transl Med.* 2012;4(115):115ra3. doi: 10.1126/scitranslmed.3002977.
31. Ma L, Young J, Prabhala H, Pan E, Mestdagh P, Muth D, et al. miR-9, a MYC/MYCN-activated microRNA, regulates E-cadherin and cancer metastasis. *Nat Cell Biol.* 2010;12(3):247-56. doi: 10.1038/ncb2024.
32. Hardee ME, Zagzag D. Mechanisms of glioma-associated neovascularization. *AmJPathol.* 2012;181(4):1126-41.
33. Gargini R, Segura-Collar B, Herranz B, Garcia-Escudero V, Romero-Bravo A, Nunez FJ, et al. The IDH-TAU-EGFR triad defines the neovascular landscape of diffuse gliomas. *SciTranslMed.* 2020;12(527).
34. Sharma S, Goswami R, Zhang DX, Rahaman SO. TRPV4 regulates matrix stiffness and TGFβ1-induced epithelial-mesenchymal transition. *J Cell Mol Med.* 2019;23(2):761-74. doi: 10.1111/jcmm.13972.
35. Gargini R, Segura-Collar B, Sánchez-Gómez P. Cellular Plasticity and Tumor Microenvironment in Gliomas: The Struggle to Hit a Moving Target. *Cancers (Basel).* 2020;12(6). doi: 10.3390/cancers12061622.
36. Soucek L, Whitfield J, Martins CP, Finch AJ, Murphy DJ, Sodikin NM, et al. Modelling Myc inhibition as a cancer therapy. *Nature.* 2008;455(7213):679-83. doi: 10.1038/nature07260.
37. Beaulieu ME, Jauset T, Massó-Vallés D, Martínez-Martín S, Rahl P, Maltais L, et al. Intrinsic cell-penetrating activity propels Omomyc from proof of concept to viable anti-MYC therapy. *Sci Transl Med.* 2019;11(484). doi: 10.1126/scitranslmed.aar5012.

- 1 38. Annibaldi D, Whitfield JR, Favuzzi E, Jauset T, Serrano E, Cuartas I, et al. Myc inhibition is
2 effective against glioma and reveals a role for Myc in proficient mitosis. *Nature*
3 *Communications*. 2014;5(1):4632. doi: 10.1038/ncomms5632.
- 4 39. Gerhardt H, Golding M, Fruttiger M, Ruhrberg C, Lundkvist A, Abramsson A, et al. VEGF
5 guides angiogenic sprouting utilizing endothelial tip cell filopodia. *The Journal of cell biology*.
6 2003;161(6):1163-77. doi: 10.1083/jcb.200302047.
- 7 40. Akeson A, Herman A, Wiginton D, Greenberg J. Endothelial cell activation in a VEGF-A
8 gradient: relevance to cell fate decisions. *Microvasc Res*. 2010;80(1):65-74. doi:
9 10.1016/j.mvr.2010.02.001.
- 10 41. Bautch VL. VEGF-directed blood vessel patterning: from cells to organism. *Cold Spring Harb*
11 *Perspect Med*. 2012;2(9):a006452. doi: 10.1101/cshperspect.a006452.
- 12 42. Whitfield JR, Soucek L. Tumor microenvironment: becoming sick of Myc. *Cell Mol Life Sci*.
13 2012;69(6):931-4. doi: 10.1007/s00018-011-0860-x.
- 14 43. Meitar D, Crawford SE, Rademaker AW, Cohn SL. Tumor angiogenesis correlates with
15 metastatic disease, N-myc amplification, and poor outcome in human neuroblastoma. *J Clin*
16 *Oncol*. 1996;14(2):405-14. doi: 10.1200/jco.1996.14.2.405.
- 17 44. Cheng L, Huang Z, Zhou W, Wu Q, Donnola S, Liu JK, et al. Glioblastoma stem cells generate
18 vascular pericytes to support vessel function and tumor growth. *Cell*. 2013;153(1):139-52.
- 19 45. Segura-Collar B, Garranzo-Asensio M, Herranz B, Hernández-SanMiguel E, Cejalvo T, Casas
20 BS, et al. Tumor-derived pericytes driven by EGFR mutations govern the vascular and immune
21 microenvironment of gliomas. *Cancer Res*. 2021. doi: 10.1158/0008-5472.can-20-3558.
- 22 46. Hooglugt A, van der Stoel MM, Boon RA, Huveneers S. Endothelial YAP/TAZ Signaling in
23 Angiogenesis and Tumor Vasculature. *Front Oncol*. 2020;10:612802. doi:
24 10.3389/fonc.2020.612802.
- 25 47. Bhat KP, Salazar KL, Balasubramaniyan V, Wani K, Heathcock L, Hollingsworth F, et al. The
26 transcriptional coactivator TAZ regulates mesenchymal differentiation in malignant glioma.
27 *Genes Dev*. 2011;25(24):2594-609.
- 28 48. Han H, Jain AD, Truica MI, Izquierdo-Ferrer J, Anker JF, Lysy B, et al. Small-Molecule MYC
29 Inhibitors Suppress Tumor Growth and Enhance Immunotherapy. *Cancer Cell*. 2019;36(5):483-
30 97.e15. doi: 10.1016/j.ccell.2019.10.001.
- 31 49. Wang N, Jain RK, Batchelor TT. New Directions in Anti-Angiogenic Therapy for
32 Glioblastoma. *Neurotherapeutics*. 2017;14(2):321-32. doi: 10.1007/s13311-016-0510-y.
- 33
34
35
36
37
38
39
40
41
42
43
44
45
46
47
48
49
50
51
52
53
54
55
56
57
58
59
60
61
62
63
64
65

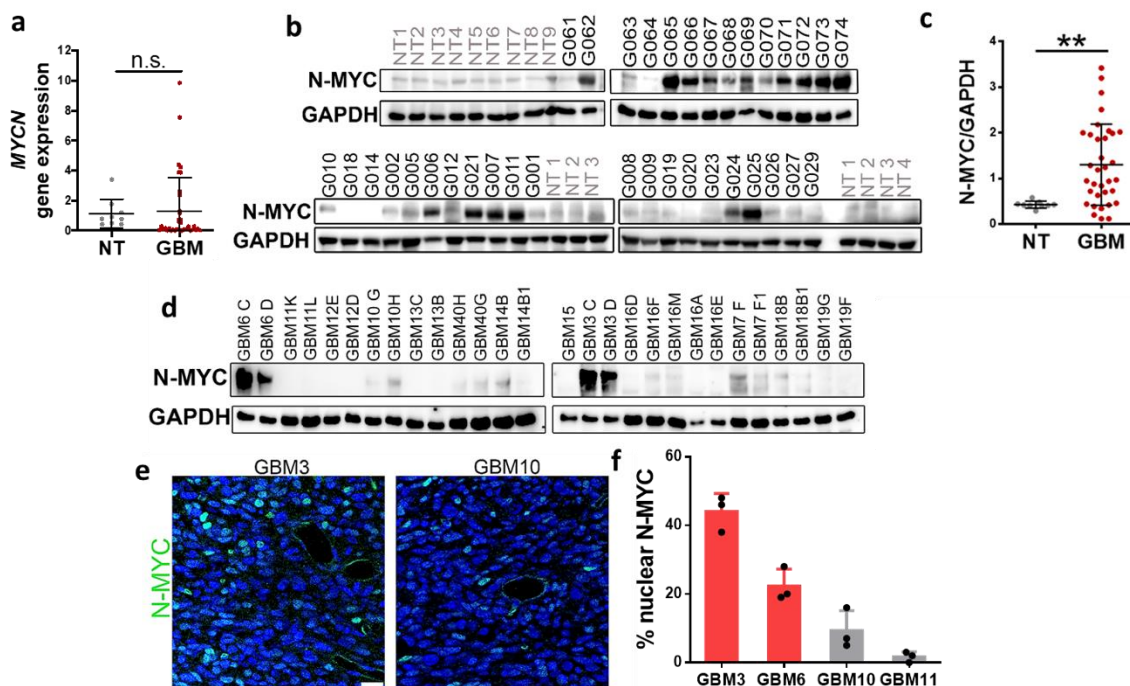


Fig 1. N-MYC expression in gliomas. **a** Quantification of *N-MYC* mRNA levels by quantitative reverse-transcriptase PCR (qRT-PCR) in a cohort of human glioblastomas (GBM) and normal brain tissues (NT) ($n = 35$ and $n = 9$). *HPRT* was used for normalization. **b-c** Western blot (WB) analysis of *N-MYC* levels in the cohort of GBM ($n = 35$) and NT ($n = 9$) and quantification in **c**. *GAPDH* was used as a loading control. **d** WB analysis of *N-MYC* levels in tumor tissue from a panel of PDXs (patient-derived xenografts). *GAPDH* was used as a loading control. **e** Representative images of the immunofluorescence staining of *N-MYC* in the PDX's tumor tissue. **f** Quantification of cells with nuclear *N-MYC* in **(e)**. ** $p < 0.01$; n.s. non-significant.

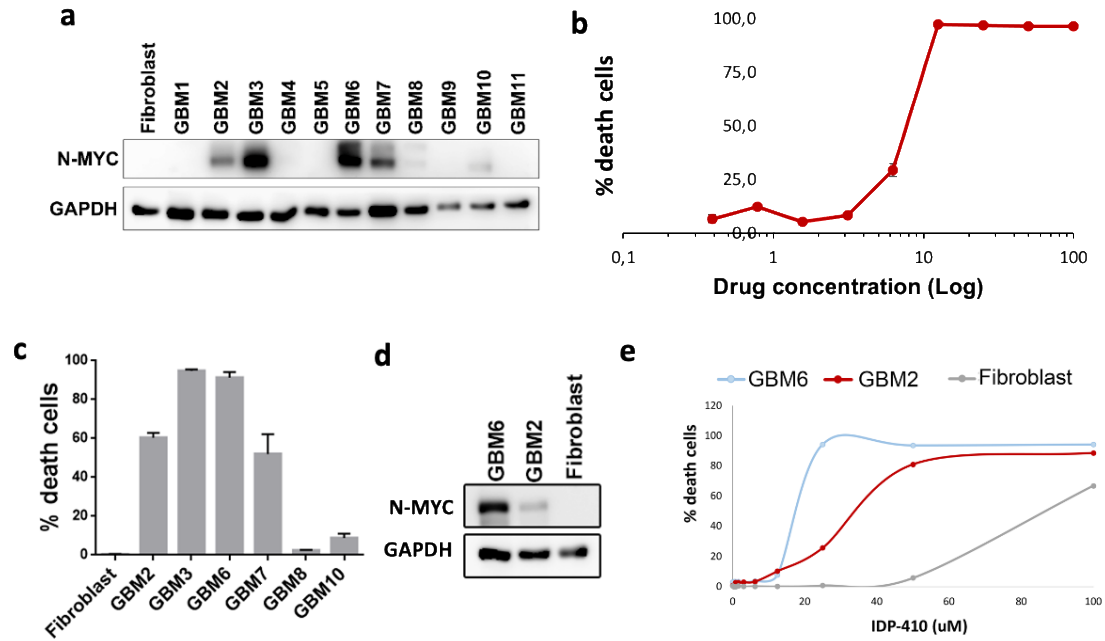


Fig 2. IDP-410 inhibits gliomas growth in vitro. **a** Western blot (WB) analysis of the levels of N-MYC in a panel of human GBM cells. Diploid human fibroblasts were used as a non-tumor control. GAPDH was used as a loading control. **b** Determination of the percentage of cell death in GBM6 cells exposed to increasing concentrations of IDP-410. **c** Analysis of the percentage of dead cells after IDP-410 treatment of a panel of human GBM cells. **d** WB showing N-MYC levels in human GBM6, GBM2 and fibroblasts. GAPDH was used as a loading control. **e** Analysis of cell death in the presence of increasing concentrations of IDP-410 in glioma cells with high (GBM6), low (GBM2) or no (fibroblasts) N-MYC expression.

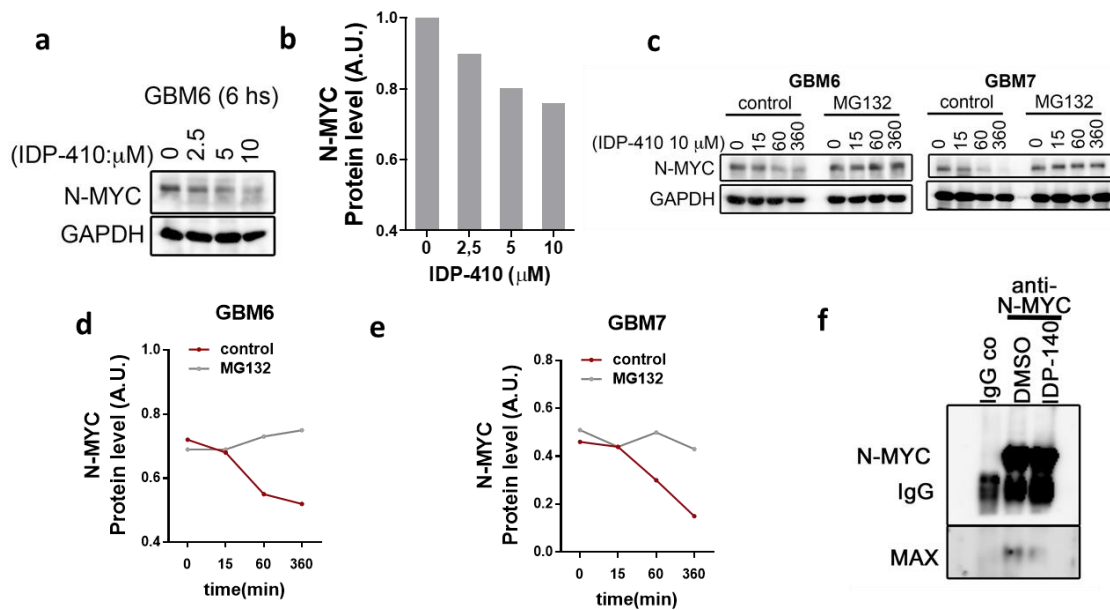


Fig 3. IDP-410 induces N-MYC degradation. **a-b** Western blot (WB) (a) and quantification (b) of N-MYC levels in GBM6 cells treated for 6h with increasing IDP-410 concentrations. GAPDH was used as a loading control. **c** WB analysis of N-MYC expression in GBM6 and GBM7 cells, incubated for different times in the presence of IDP-410 (10 μM), with or without the proteasome inhibitor MG132 (20 μM). GAPDH was used as a loading control. **d-e** Quantification of the WB in (c) for GBM6 (d) and GBM7 (e) cells. **f** Extracts from GBM6 cells, incubated in the presence of DMSO or IDP-410, were immunoprecipitated (IP) using anti-N-MYC antibodies. The IP fractions were analyzed by WB with N-MYC and MAX antibodies. Control IP with IgG is shown on the left lane.

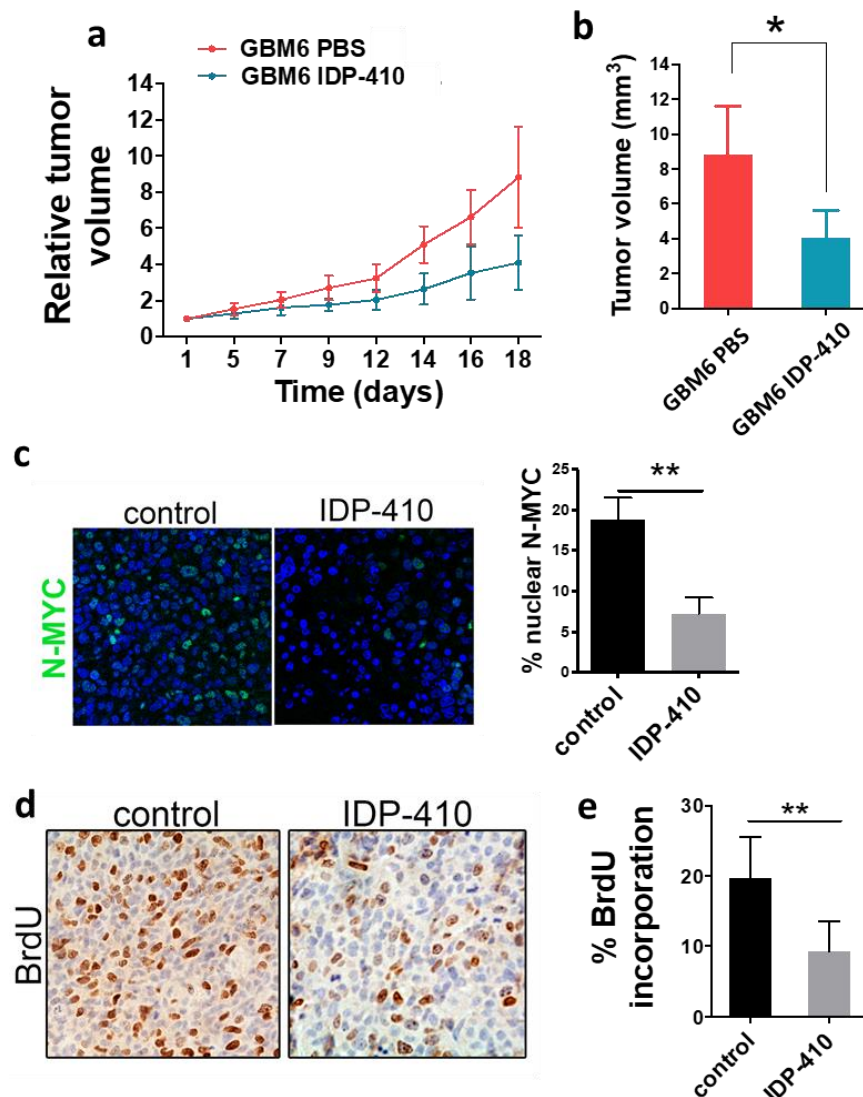


Fig 4. Systemic IDP-410 impairs the subcutaneous growth of gliomas. **a** Growth curve of GBM6 cells implanted in the flank of nude mice, which were treated by bolus intravenous route (i.v.) with vehicle or IDP-410 twice a week (dose 15 mg/kg). **b** Determination of the tumor volume at the final end point in (a). **c** Representative images of the immunofluorescence analysis of nuclear N-MYC in tumors treated with vehicle (control) or IDP-410. Quantification is shown on the right. **d-e** Determination of tumor cell proliferation measured by incorporation of BrdU and quantified using immunohistochemistry in tumors treated with vehicle (control) or IDP-410. * $p < 0.05$; ** $p < 0.01$.

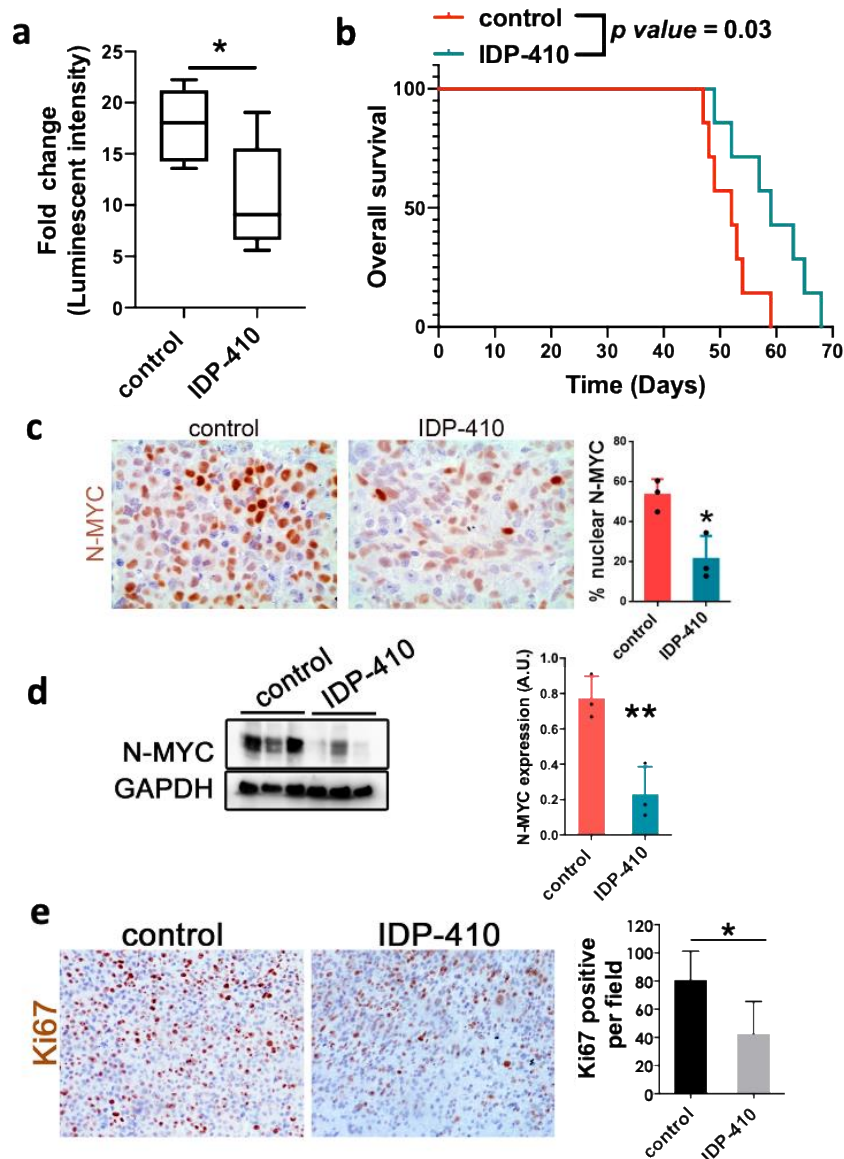


Fig 5. Systemic IDP-410 impairs the intracranial growth of gliomas. **a** GBM6 cells were intracranially injected in Nude mice and the animals were treated with vehicle (control) or IDP-410 (15mg/Kg; 5 days a week). The graph shows the fold increase in luminescence (between day 40 and day 52 after cell injection) in control and IDP-410 treated mice. **b** Kaplan-Meier survival curve of GBM6-bearing mice treated with vehicle (control) or IDP-410. **c** Representative pictures of the immunohistochemical (IHC) staining of N-MYC in tumors from (b). Quantification of the nuclear N-MYC staining is shown on the right (n=3/condition). **d** Western blot of N-MYC levels in GBM6 intracranial tumors from (b). GAPDH was used as a loading

control. Quantification is shown on the right (n=3/condition). **e** Representative pictures of IHC staining of Ki67 in tumors from (b). Quantification is shown on the right (n=3/condition). *p < 0.05, **p < 0.01.

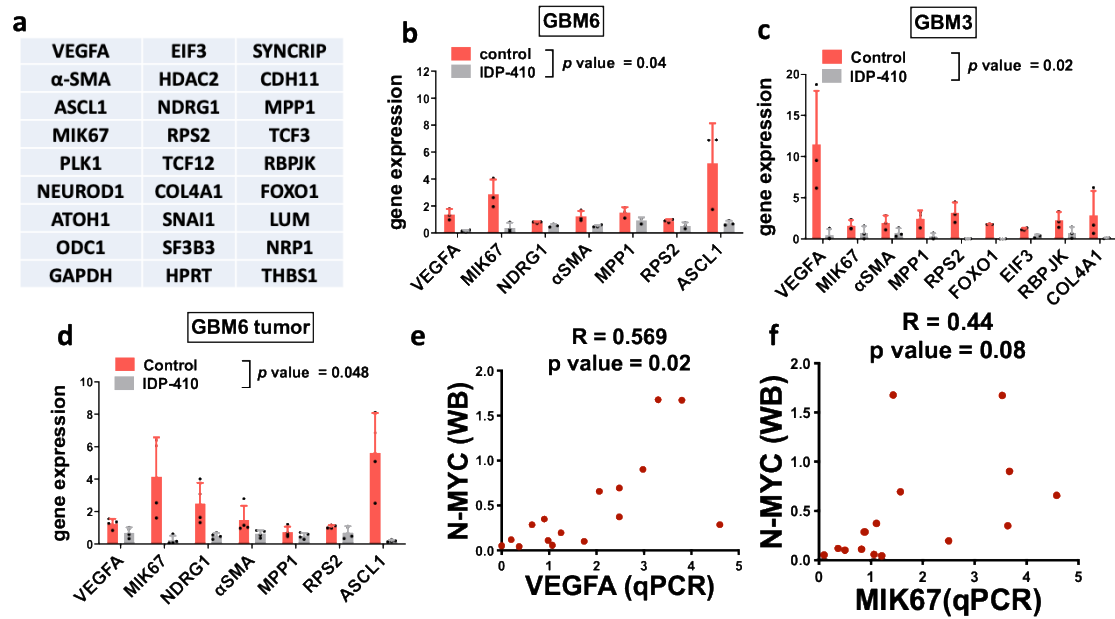


Fig 6. Effect of IDP-410 in proliferation and angiogenesis-related genes regulated by N-MYC in gliomas. a N-MYC upregulated gene signature. **b-c** Quantitative reverse-transcriptase PCR (qRT-PCR) analysis of several *N-MYC*-related genes (from a) in GBM6 (b) and GBM3 (c) cells treated with vehicle (control) or IDP-410. *HPRT* was used for normalization. **d** qRT-PCR analysis of a signature of *N-MYC*-related genes in GBM6 intracranial tumors from Fig 5. **e-f** Pearson's correlation analysis between the expression of *VEGFA* (d) and *MKI67* (e) and the amount of N-MYC protein in a panel of PDXs (Supplementary Fig. 3).

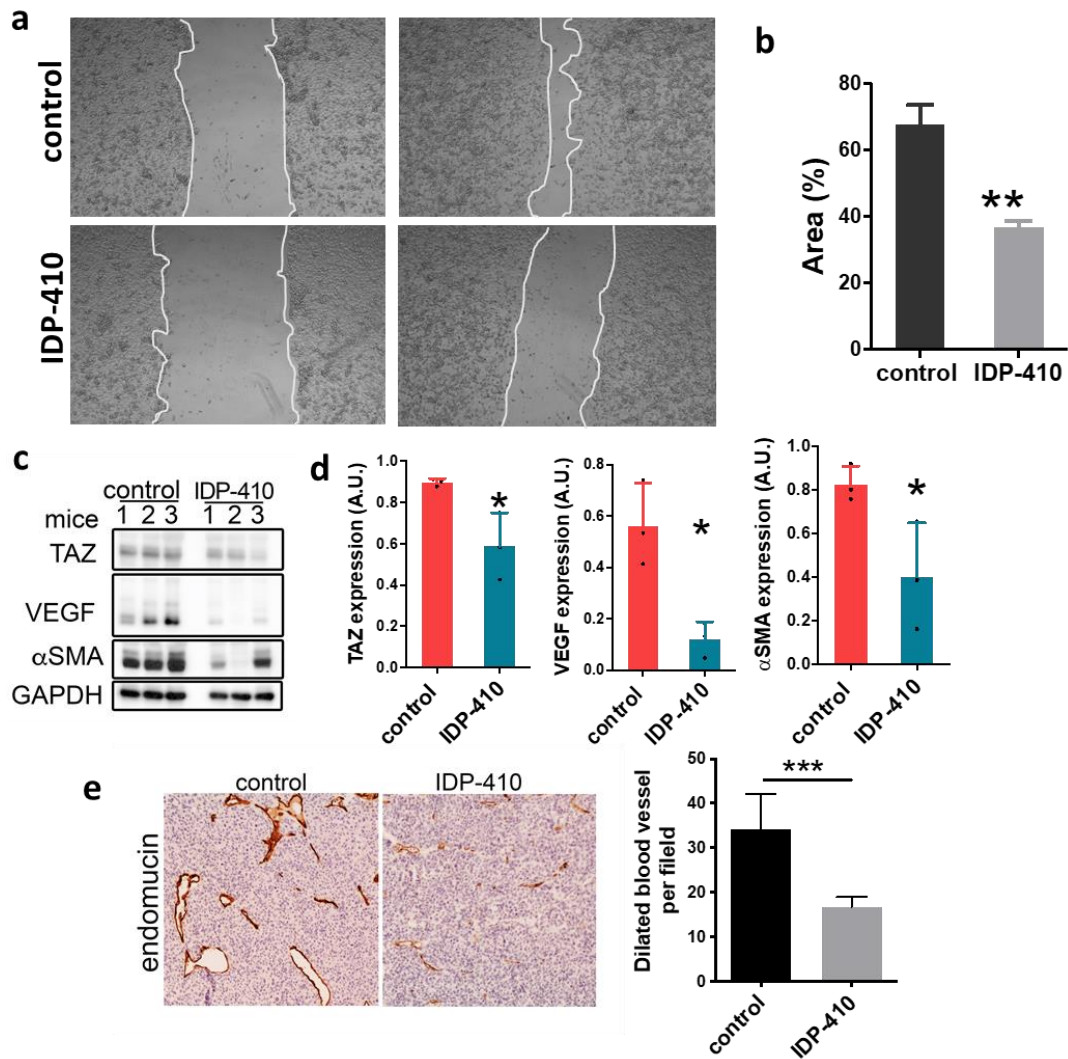


Fig 7. IDP-410 impairs vascularization of gliomas. **a** Representative images from a wound healing test of HBMEC cells incubated in the presence of conditioned media from control or IDP-410 treated GBM6 cells. **b** Quantification of the percentage of the scratch area reduction in (a). **c** Western blot analysis of TAZ, VEGF and α SMA in GBM6 tumors treated with vehicle (control) and IDP-410. GAPDH was used as a loading control. **d** Representative pictures of the immunohistochemical staining of endomucin in GBM6 control and IDP-410 tumors. Quantification is shown on the right (n=3/condition). **e** Quantification of the number of dilated blood vessels in (d) (n = 3). **p < 0.01; ***p < 0.001.



Click here to access/download
Conflict of Interest Form
Col Ricardo Gargini.pdf





Click here to access/download
Conflict of Interest Form
Col Miguel Moreno.pdf





Click here to access/download
Conflict of Interest Form
Col Laura Nevola.pdf





Click here to access/download
Conflict of Interest Form
Col Juan Manuel Sepulveda.pdf





Click here to access/download
Conflict of Interest Form
Col Daniel Lobato.pdf





Click here to access/download
Conflict of Interest Form
Col Maria Garranzo.pdf



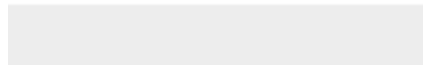


Click here to access/download
Conflict of Interest Form
Col Rafael Hortiguela.pdf





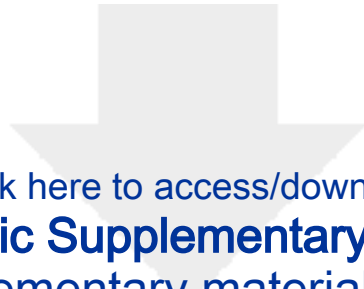
Click here to access/download
Conflict of Interest Form
Conflict of Interest Form_PSG.pdf





Click here to access/download
Conflict of Interest Form
Col Berta Segura.pdf





Click here to access/download
Electronic Supplementary Material
Supplementary materials.docx

